JATIS Journal of Astronomical Telescopes, Instruments, and Systems

RESEARCH PAPER

Synthesizing high-fidelity phase screens from the phase fluctuation correlation function

Matteo Faccioni,[a,b,*] **Daniel Kiehn**,[c] **and Patrick Vrancken**[b]

[a]Deutsches Zentrum für Luft- und Raumfahrt (DLR), Institut für Physik der Atmosphäre, Oberpfaffenhofen, Germany
[b]Technical University of Munich, Institute of Astronomical and Physical Geodesy, School of Engineering and Design, Department of Aerospace and Geodesy, Munich, Germany
[c]DLR Institute of Flight Systems, Braunschweig, Germany

ABSTRACT. In this publication, a new method for synthesizing high-fidelity phase screens is presented. The method is based on the phase fluctuations correlation function; hence, it is called correlation-based random phase method. By synthesizing the phase screens from a function defined in the spatial domain (i.e., the correlation function) rather than in the frequency domain, the bandwidth error arising while using a single discrete Fourier transform is corrected, allowing the synthesization of phase screens yielding a negligible deviation from the theoretical structure function without the need of any optimization parameters. Originally developed in the field of aeronautics, the correlation-based random phase method is limited by computer arithmetic inaccuracies for grid size that are around 4 times larger than the considered outer scale, an assumption that is often valid while simulating the effects of a turbulent atmosphere on ground-based astronomical telescopes with a large aperture. It is possible to achieve the same accuracy in the case of smaller spatial domains by applying a proper window function, at the cost of increasing the number of pixels (i.e., the computation time). For illustration, the presented method is compared with the widely known random phase method.

 [DOI: 10.1117/1.JATIS.12.3.039002]

Keywords: optical propagation; correlation function; phase screens

Paper 260118 received May 19, 2026; revised Jul. 28, 2026; accepted Aug. 10, 2026; published Aug. 27, 2026.

1 Introduction

Propagation of electromagnetic waves in a turbulent media has been, and continues to be, extensively studied over the last sixty years[1–3] due to its importance in different fields, from free space optical communication[4] to astronomy.[5] In particular, within a few years, a new class of ground astronomical telescopes, all with an aperture larger than 20 m[6–8] will become operational allowing to investigate the wonders of our universe at a resolution never seen before. In this context, it is essential to quantify the effects of the Earth turbulent atmosphere on the incoming starlight.[9] In fact, the turbulent motion of the atmosphere causes temperature gradients that cause fluctuations in the refractive index of the air, acting on the propagating wave as multiple lenses with different optical powers and inclinations.[10] It is possible to express how the refractive index fluctuations are distributed at different wavenumbers by means of the refractive index fluctuations power spectral density (PSD), Φ_n. The latter, assuming a von Kármán (VK) spectrum and a 3D domain, can be written as follows[1]:

*Address all correspondence to Matteo Faccioni, matteo.faccioni@dlr.de

$$\Phi_n(\kappa) = 0.033 C_n^2 (\kappa^2 + \kappa_0^2)^{-11/6}, \tag{1}$$

where $\kappa = |\boldsymbol{\kappa}|$ is the magnitude of the wavenumber vector, C_n^2 is the refractive index structure constant describing the strength of the turbulence, $\kappa_0 = 2\pi/L_0$, and L_0 is the outer scale of the turbulence, a quantity ranging from tens to hundreds of meters in the Earth atmosphere.[11] To quantify the effects of a turbulent atmosphere on a propagating electromagnetic wave, it is more convenient to express the turbulence strength with the Fried parameter r_0, a quantity having the dimension of length and corresponding to the diameter of a heterodyne receiver at which turbulence begins to seriously limit its performance.[12] In the case of a propagating plane wave, the Fried parameter is[13]:

$$r_0 = \left[0.423\left(\frac{2\pi}{\lambda}\right)^2 (\cos\,\theta)^{-1} \int_0^{\zeta} C_n^2(z)\mathrm{d}z\right]^{-3/5}, \tag{2}$$

where λ is the wavelength of the wave, θ is the zenith angle of the receiver, and ζ is the propagation distance. Finally, assuming an isotropic turbulent field, the 2D phase fluctuations PSD $\phi_\vartheta(\kappa)$, is related with Φ_n by the following expression[14]:

$$\phi_\vartheta(\kappa) = 0.49 r_0^{-5/3} (\kappa^2 + \kappa_0^2)^{-11/6}. \tag{3}$$

Having statistically quantified the phase fluctuations generated by the turbulent atmosphere, and assuming Taylor's hypothesis of frozen turbulence to hold,[15] it is possible to simulate the wave propagation in a turbulent atmosphere using the phase screen method.[16] This approach consists in dividing the propagation path into different segments, and simulating, for each segment, the phase fluctuations induced by the turbulent atmosphere through a 2D phase screen. The wave is then propagated sequentially from one screen to the next, until its entire path is simulated. The phase screens can be synthesized using several methods based on different statistical approaches, including autoregressive models,[17] machine learning,[18] modal decomposition techniques,[19] the spectral representation of the phenomenon,[16] or a combination of the last two.[20] Of all these approaches, the most commonly used is the spectral representation method, referred to in this publication as *random phase method* (RPM) after Wilson,[21] in which the phase screens are synthesized starting from the phase fluctuations PSD. However, being the bandwidth of the PSD not finite in the considered spatial domain, the RPM introduces an error both at the small and large scales.[22,23] To solve this issue various solutions have been proposed, such as the subharmonics method,[23] a modal decomposition of the correlation function,[24] or a family of methods relying on the sparse spectrum model of the phase fluctuations.[25] The first two approaches require to compute specific optimization parameters for each simulation, whereas the latter class of methods synthesize the phase screens with a low error (i.e., of the order of 0.1%) by sampling the phase fluctuations PSD at random wavenumbers.

The objective of this work is to introduce the use of the correlation-based random phase method (CB-RPM) for synthesizing the phase screens. This approach, being *exact in principle*[26] (i.e., the error of the method is limited by the computer arithmetic inaccuracies), allows correcting for the errors of the RPM both at the small and large scales for spatial domains greater than $4L_0$, often a valid assumption for the new class of large aperture ground telescopes. This high degree of accuracy is achieved using the relation between the correlation function and the PSD (i.e., the two quantities being a Fourier pair). However, the method is limited at smaller spatial scales due to the occurrence of negative values in the PSD. To solve this issue, it is proposed to mask the phase fluctuations structure function with a proper window, improving the CB-RPM accuracy even at smaller scales at the cost of increasing the number of pixels in the spatial grid and the computation time.

This publication is structured as follows: in Sec. 2, the theory behind the RPM is presented. The verification procedure of the synthesized phase screens is described in Sec. 3, whereas the CB-RPM is presented in Sec. 4. In Sec. 5, it is explained how to obtain high-fidelity screens even at small spatial scales while using the CB-RPM, and the conclusions are presented in Sec. 6.

2 Synthesizing the Phase Screens Using the RPM

First applied by Shinozuka and Jan[27] in the field of structural analysis, in the last two decades, the RPM has been widely used to model the effects of a turbulent atmosphere on long distant sources.[14,16,28,29] The RPM synthesization of a single 2D phase screen ϑ_{RPM} is expressed as follows:

$$\vartheta_{\mathrm{RPM}} = \mathrm{Re}/\mathrm{Im}\left\{\mathcal{F}^{-1}\left(\mu\frac{2\pi}{\sqrt{L_x L_y}}N_x N_y\sqrt{\phi_\vartheta(\kappa)}\right)\right\}, \tag{4}$$

where L_i is the domain size of the i'th axis, Re/Im means that either the real or imaginary component of the result can be used, N_i is the number of pixels of the i'th axis, $\mathcal{F}^{-1}$ stands for the inverse Discrete Fourier transform (IDFT), and μ is a set of complex random variables with zero mean and unit variance. Figure 1 shows a phase screen synthesized using Eq. (4), considering a spatial domain $L_x = L_y = 60$ m, a Fried parameter $r_0 = 0.5$ m, a grid with $N_x = N_y = 2048$ pixels, and a turbulence outer scale $L_0 = 15$ m.

3 RPM Verification

As suggested in Johansson and Gavel,[30] to check the quality of the phase screen thus synthesized its structure function D is compared with the theoretical one. Assuming a 2D VK phase fluctuation spectrum, the theoretical phase fluctuation structure function is as follows[31]:

$$D_\vartheta(r) = 6.16\, r_0^{-5/3}\left[\frac{3}{5}\kappa_0^{-5/3} - \left(\frac{r}{2\kappa_0}\right)^{5/6}\frac{K_{5/6}(\kappa_0 r)}{\Gamma(11/6)}\right], \tag{5}$$

where Γ is the gamma function, K_ν is the modified Bessel function of the second kind, and $r = |\boldsymbol{r}|$ is the magnitude of the separation vector. The error of the synthesized phase screen is then computed as follows:

$$\epsilon(r) = |D(r) - D_\vartheta(r)|. \tag{6}$$

Analyzing the RPM error represented in Fig. 2, it is clear that the synthesized phase screen does not perfectly represent the required statistics, underestimating the phase fluctuations both at the high and the low wavenumbers. This error arises due to the fact that the PSD is not a

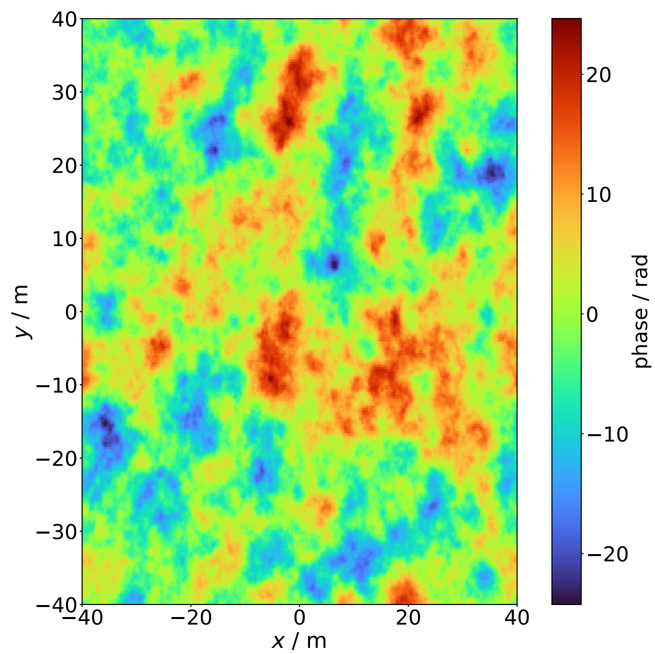

Fig. 1 Phase screen synthesized using the RPM. A VK spectrum is assumed, considering $r_0 = 0.5$ m, $L_x = L_y = 60$ m, $N_x = N_y = 2048$, and $L_0 = 15$ m.

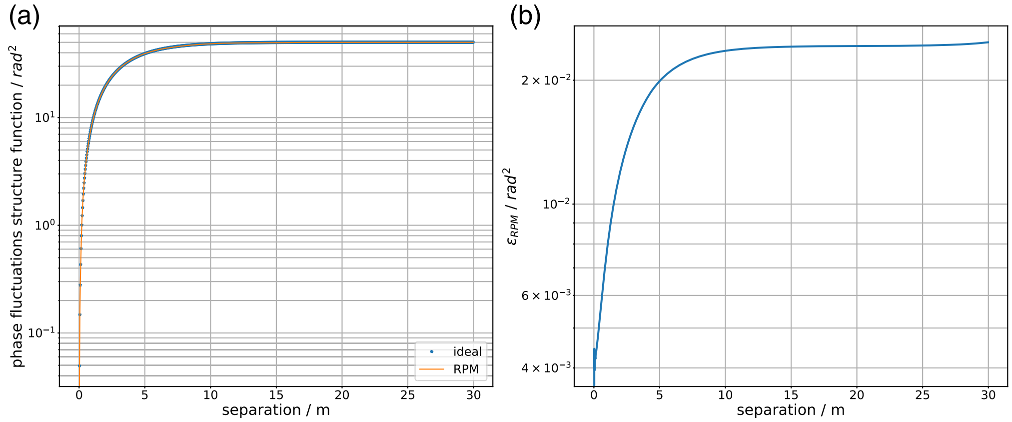

Fig. 2 (a) Comparison between the expected RPM structure function and the theoretical one. Theoretical structure function in blue stars, RPM expected structure function in orange line. (b) Error $\varepsilon_{\mathrm{RPM}}$ of the expected RPM structure function with respect to the theoretical one.

bandwidth-limited function in the desired wavenumber domain, consequently the implementation of the discrete Fourier transform (DFT) generates a sampling error, as stated in the Nyquist-Shannon sampling theorem.[22] Various methods have been proposed to solve this problem. These include the *sub-harmonic method*,[23] which decreases the inaccuracies in the low-wavenumber region by replacing the single sample at the origin in the wavenumber domain by nine (or even more) sub-samples, and a modal decomposition of the correlation function,[24] where the phase correlation function is preprocessed by extracting the piston and tilt components and then a mask is applied. However, these methods are not of general nature (i.e., they cannot be applied for all kinds of PSDs), and it is needed to compute different optimization parameters from spatial domain to spatial domain. Another families of methods that solve this error are based on the sparse spectrum of the phase fluctuations,[25,32,33] achieving a low error (i.e., of the order of 0.1%) at the same computation time of the fourth-order sub-harmonic method.

Whether this error is small enough to be neglected must be assessed on a case-by-case basis. Considering the phase fluctuations over different phase screens to be uncorrelated,[34] the phase underestimation at the pupil can be roughly quantified as the square of the product between the maximum value of the error ε and the number of phase screens P:

$$\Delta_{\vartheta} \sim \sqrt{P\varepsilon_{\mathrm{max}}}. \tag{7}$$

Two criteria to quantify the error committed in the simulation are proposed in Faccioni et al.[35] These are respectively, the point spread function (PSF) (i.e., the Fourier transform of the system's entrance pupil in the case of an incoming plane wave), and the Zernike power spectrum[36] of the wavefront at the entrance pupil. Additionally, in order to understand how the error committed in the simulation depends on different simulation scenario, it is convenient to consider the error ε as an additional phase screen, characterized by the Fried parameter $r_{0,\varepsilon}$ and the outer scale $L_{0,\varepsilon}$. As the turbulence intensity increases (i.e., in the case of a smaller Fried parameter, or a greater outer scale) and the number of phase screens remains unchanged, the error ε increases, leading to a less accurate simulation, modeling a narrower PSF and a lower Zernike power spectrum of the wavefront at the entrance pupil, underestimating the modes that an adaptive optics system shall correct. At the moment it does not exist a general expression assessing the error committed in the simulation from the turbulence parameters, hence the estimation of the accuracy of the simulation and whether the committed error can be neglected must be evaluated on a case-by-case basis.

4 Synthesizing the Phase Screens Using the CB-RPM

The CB-RPM has been developed with the aim of eliminating the bandwidth error arising while using the RPM. This is done by taking advantage of the relation between the correlation function and the PSD (i.e., the two quantities being a Fourier pair as stated in the Wiener–Khinchin

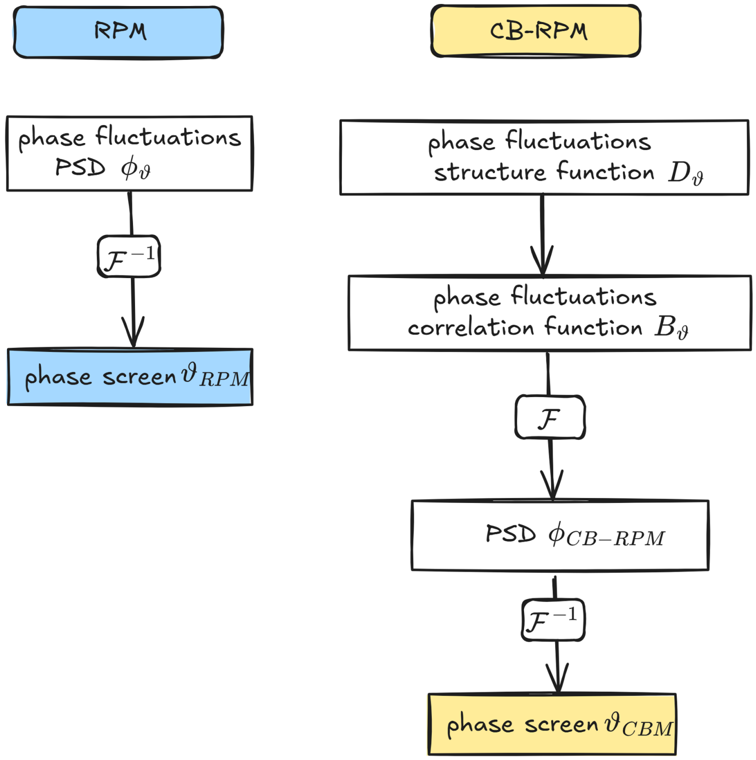

Fig. 3 RPM flowchart in blue. CB-RPM flowchart in yellow.

theorem[37]). By computing the phase fluctuations PSD as the DFT of the theoretical phase fluctuations correlation function B_θ, the latter being defined on the spatial domain $\boldsymbol{s}$, the bandwidth error is indeed eliminated. The flowcharts of the two methods are represented in Fig. 3.

The phase screen $\vartheta_{\text{CB-RPM}}$ obtained using the CB-RPM is:

$$\vartheta_{\text{CB-RPM}} = \text{Re}/\text{Im}\left\{\mathcal{F}^{-1}\left(\mu\sqrt{\mathcal{F}(B_\vartheta(r))N_x N_y}\right)\right\}, \tag{8}$$

where $B_\vartheta(r)$ is the theoretical phase fluctuations correlation function, computed from the theoretical structure function expressed in Eq. (5) as follows[1]:

$$B_\vartheta(r) = \frac{1}{2}[D_\vartheta(\infty) - D_\vartheta(r)]. \tag{9}$$

Figure 4 shows a phase screen synthesized using the CB-RPM considering the same values of Sec. 2, and its error $\varepsilon_{\text{CB-RPM}}$. The extremely low error of the expected CB-RPM structure function demonstrates how the method allows to synthesize phase screens that respect the desired statistics being *exact in principle* for spatial domains greater than $4L_0$. Its exactness refers to the computational errors, not to how close the synthesized phase screen simulates reality. However, using a method that does not introduce computational errors would allow to refine the phase screens synthesis considering PSDs obtained from real data taking into account the refractive index field anisotropies,[38] and non-Kolmogorov turbulence.[39] In fact, phase screens are generally synthesized assuming a homogeneous and isotropic turbulence, however, especially for turbulence near the surface, this assumption is no longer valid.[40] As a final remark to this section, the authors considered to be more appropriate to compare the synthesized phase screens correlation functions than their PSDs. This is done to avoid biases generated by computing the PSDs using the DFT or the power underestimation in the phase screens power due to windowing.[41]

5 Reducing the CB-RPM Error at Smaller Spatial Scales

Similarly to the function ϕ_{FFT} presented in Xiang[24] the PSD computed using the CB-RPM $\phi_{\text{CB-RPM}}(\kappa)$ yields negative values for spatial domains smaller than $4L_0$. This is theoretically

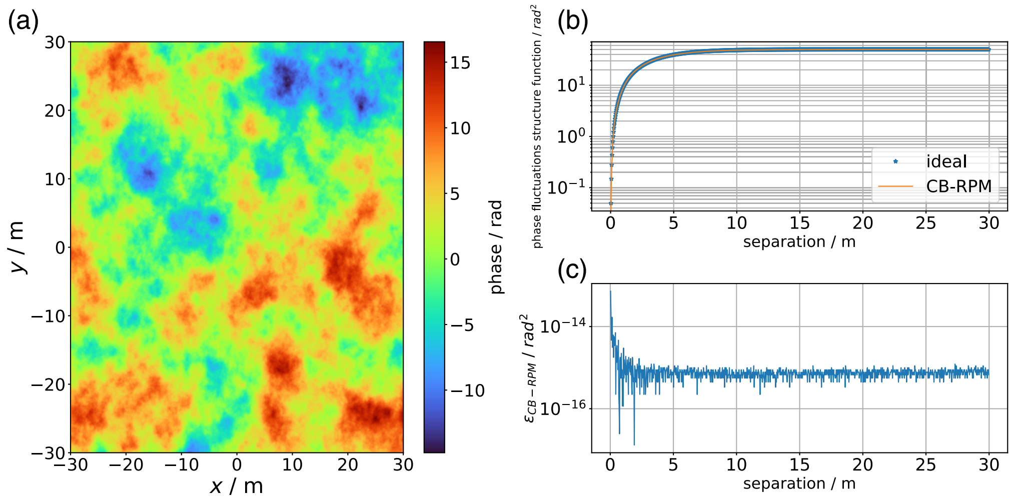

Fig. 4 (a) Phase screen synthesized using the CB-RPM. A VK spectrum is assumed, considering $r_0 = 0.5$ m, $L_x = L_y = 60$ m, $N_x = N_y = 2048$, and $L_0 = 15$ m. (b) Comparison between the expected CB-RPM structure function and the theoretical one. Theoretical structure function in blue stars, expected CB-RPM structure function in orange line. (c) Error $\varepsilon_{\mathrm{CB-RPM}}$ of the expected CB-RPM structure function with respect to the theoretical one.

incorrect, because the PSD is defined as a positive function. The occurrence of these negative values is due to the implementation of the DFT for very small spatial domains, scales for which the correlation function becomes almost flat and to synthesize the desired correlation function some of the DFT coefficients are phase-shifted by a factor π (i.e., having negative-amplitude values). Considering the extreme case of an uniform circular correlation function, its Fourier transform is a *jinc* function,[42] demonstrating how the appearance of negative values in the $\phi_{\mathrm{CB-RPM}}$ is expected for specific shapes of the correlation function. To overcome this issue and eliminate the arise of negative values in the PSD, it is proposed to enlarge the spatial domain of the simulation and to window part of the theoretical structure function in the region of no-interest. This is done using the error function erf as window and adding the peak value F at the edge of the window. The resulting structure function substituting the theoretical structure function in Eq. (9) is:

$$D_{\mathrm{CB-RPM}}(r) = D_{\vartheta}(r)(1 - \mathrm{erf}(A)) + 6.16 r_0^{-5/3} F \mathrm{erf}(A), \tag{10}$$

where $A = \{[(r - r_t C)E] + 1\}/2$ and r_t is the spatial grid radius of interest. The result obtained considering a spatial domain of $Dx = Dy = 20$ m, a turbulence outer scale $L_0 = 60$ m, a Fried parameter $r_0 = 0.5$ m, $Nx = Ny = 128$, and the values for $D_{\mathrm{CB-RPM}}$ listed in Table 1, is presented in Fig. 5. The usage of the proposed window allows the CB-RPM to be exact in principle even for spatial domains smaller than $4L_0$, allowing to model the viscosity effects arising at scales of the order of the turbulence inner scale l_0.[1] The drawback of windowing is the need for a larger number of pixels, causing an increased computation time for each DFT of $M \cdot (1 + \log(M/N)/\log(N))$, where M and N are the new and old number of pixels of the grid respectively.

Table 1 $D_{\mathrm{CB-RPM}}$ parameters.

Parameter	Value
r_t	10
C	3
E	0.3
F	23

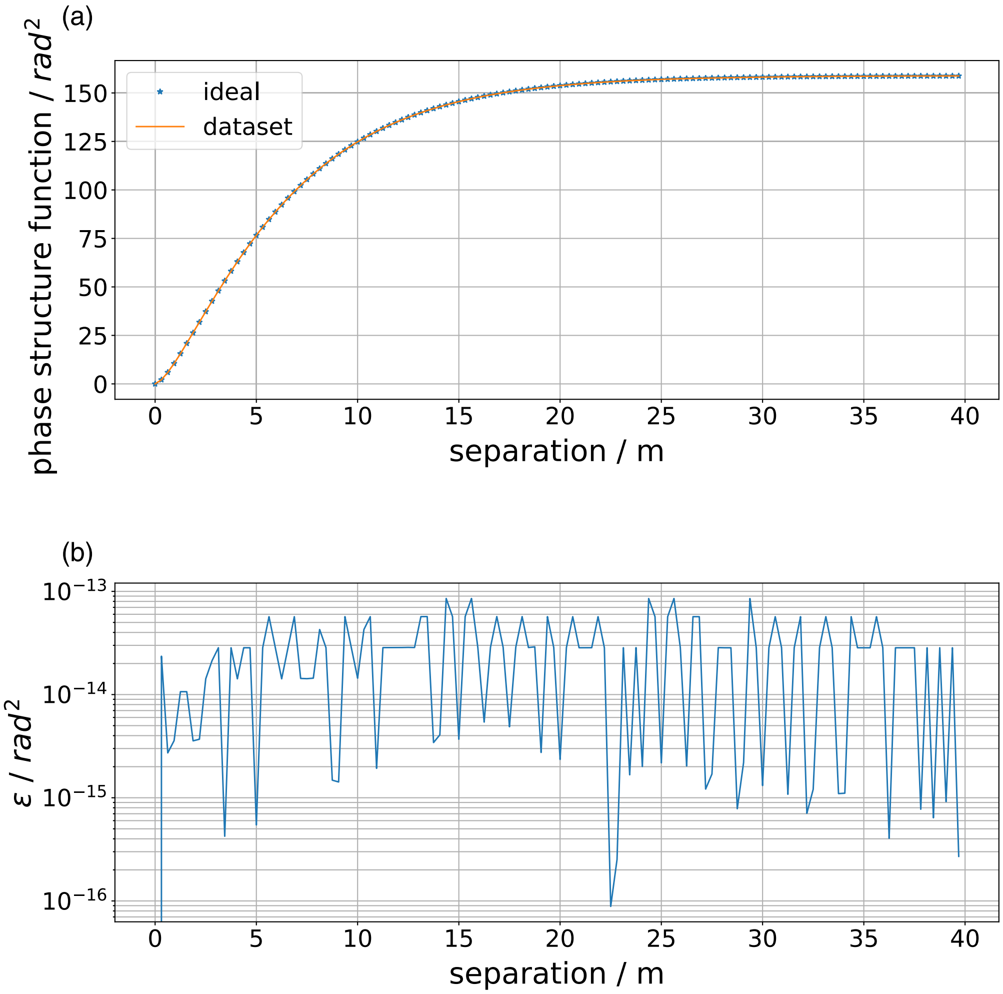

Fig. 5 (a) Comparison between the different methods phase screens structure functions and the theoretical one. Theoretical structure function in black stars, expected RPM structure function in blue line, expected CB-RPM structure function in dashed orange line. (b) Errors of the different methods' expected structure functions with respect to the theoretical one. RPM error $\varepsilon_{\mathrm{RPM}}$ in blue line, and CB-RPM error $\varepsilon_{\mathrm{CB-RPM}}$ in dashed orange line.

6 Conclusion

In this publication, a new high-fidelity method for synthesizing phase screens has been presented. This new approach, called CB-RPM, allows to obtain a more accurate phase screen as compared with the RPM without the need of any optimization parameters for spatial domains larger than $4L_0$. Two criteria are proposed to assess whether the error committed while using the RPM or other methods can be neglected os shall be addressed using the CB-RPM. In addition, the latter is exact in principle also for rectangular spatial domains, an interesting result that can be applied to represent the effects of a turbulent atmosphere on a long and narrow beam, such as the one emitted by a laser guide star. With the proper window, the CB-RPM is exact in principle also at smaller scales, allowing to synthesize high-fidelity phase screens considering also the dissipation effect due to viscosity.

Disclosures

The authors declare that there are no financial interests, commercial affiliations, or other potential conflicts of interest that could have influenced the objectivity of this research or the writing of this paper.

Code and Data Availability

Data sharing is not applicable to this article, as no new data were created or analyzed.

Acknowledgments

The authors would like to acknowledge Dr Bruno Femenia Castella (OHB, formerly DLR) insightful comments and for the nice and interesting bilingual lunches in Oberpfaffenhofen, and Dr Alex Barnett (Flatiron Institute) for the wise suggestion regarding the impossibility of implementing the nonuniform fast Fourier transform (NUFFT) to correct for the negative values appearing in the PSD computed in the CB-RPM. The authors acknowledge particularly the suggestions of the anonymous reviewers that greatly increased the quality of the publication. Many thanks for your time.

References

1. V. I. Tatarski, *Wave Propagation in a Turbulent Medium*, McGraw-Hill Book Company, Inc. (1961).
2. L. A. Chernov, *Wave Propagation in a Random Medium*, McGraw-Hill Book Company, Inc. (1961).
3. M. Kalensky et al., "Aero-optical effects, part I. System-level considerations: tutorial," *J. Opt. Soc. Am.* **41**, 2163 (2024).
4. L. C. Andrews and R. L. Phillips, *Laser Beam Propagation Through Random Media*, SPIE Press, Bellingham, Washington (2005).
5. A. Boné, C. Delacroix, and O. Absil, "Simulating the effect of chromatic beam wander on the ELT/METIS high-contrast imaging performance," *J. Astron. Telesc. Instrum. Syst.* **12**, 014001 (2026).
6. ESO, "The E-ELT design reference mission," Technical report E-TRE-ESO-080-0717 Issue 2, ESO (2011).
7. GMTO, "Giant Magellan Telescope science book 2018," Technical report, GMTO (2018).
8. TIO, "TIO detailed science case: 2024," Technical report TIO.PSC.TEC.07.007.CCR04, TIO (2024).
9. B. L. Ellerbroek and G. Cochran, "Wave optics propagation code for multiconjugate adaptive optics," *Proc. SPIE* **4494**, 104–120 (2002).
10. S. F. Clifford, *The Classical Theory of Wave Propagation in a Turbulent Medium*, pp. 9–43, Springer Berlin Heidelberg (1978).
11. V. P. Lukin, "Outer scale of atmospheric turbulence," *Proc. SPIE* **5981**, 598101 (2005).
12. D. L. Fried, "Optical heterodyne detection of an atmospherically distorted signal wave front," *Proc. IEEE* **55**(1), 57–77 (1967).
13. F. Roddier, "The effects of atmospheric turbulence in optical astronomy," in *Progress in Optics*, Vol. **XIX**, pp. 281–376 (1981).
14. J. D. Schmidt, *Numerical Simulation of Optical Wave Propagation with Examples in MATLAB, SPIE*, SPIE Press, Bellingham, Washington (2010).
15. G. I. Taylor, "Statistical theory of turbulence," *Proc. R. Soc. Lond. Ser. A Math. Phys. Sci.* **151**(873), 421–444 (1935).
16. R. G. Lane, A. Glindemann, and J. C. Dainty, "Simulation of a Kolmogorov phase screen," *Waves Random Media* **2**, 209–224 (1992).
17. A. J. Baran and D. G. Infield, "Simulating atmospheric turbulence by synthetic realization of time series in relation to power spectra," *J. Sound Vib.* **180**, 627–635 (1995).
18. S. Lohani, E. M. Knutson, and R. T. Glasser, "Generative machine learning for robust free-space communication," *Commun. Phys.* **3**, 177 (2020).
19. D. L. Fried, "Statistics of a geometric representation of wavefront distortion," *J. Opt. Soc. Am.* **55**, 1427 (1965).
20. D. Bachmann et al., "Accurate Zernike-corrected phase screens for arbitrary power spectra," *Opt. Eng.* **64**(5), 058102 (2025).
21. D. K. Wilson, "Turbulence models and the synthesis of random fields for acoustic wave propagation calculations," Tech. Rep. ARL-TR-1677, US Army Research Laboratory, Adelphi, MD, USA (1998).
22. C. E. Shannon, "Communication in the presence of noise," *Proc. IRE* **37**(1), 10–21 (1949).
23. G. Sedmak, "Performance analysis of and compensation for aspect-ratio effects of fast-Fourier-transform-based simulations of large atmospheric wave fronts," *Appl. Opt.* **37**, 4605–4613 (1998).
24. J. Xiang, "Fast and accurate simulation of the turbulent phase screen using fast Fourier transform," *Opt. Eng.* **53**(1), 016110 (2014).
25. M. Charnotskii, "Comparison of four techniques for turbulent phase screens simulation," *Appl. Opt.* **37**(5), 738 (2020).
26. A. T. A. Wood and G. Chan, "Simulation of stationary Gaussian processes in $[0, 1]^d$," *J. Comput. Graph. Stat.* **3**(4), 409–432 (1994).
27. M. Shinozuka and C. M. Jan, "Digital simulation of random processes and its applications," *J. Sound Vib.* **25**, 111–128 (1972).
28. M. J. Townson et al., "AOtools: a Python package for adaptive optics modelling and analysis," *Opt. Express* **27**(22), 31316 (2019).

29. Y. K. Chanine et al., "Beam propagation through atmospheric turbulence using an altitude-dependent structure profile with non-uniformly distributed phase screens," *Proc. SPIE* **11272**, 1127215 (2020).
30. E. M. Johansson and D. T. Gavel, "Simulation of stellar speckle imaging," *Proc. SPIE* **2200**, 372–383 (1994).
31. V. P. Lukin and V. V. Pokasov, "Optical wave phase fluctuations," *Appl. Opt.* **20**(1), 121 (1981).
32. M. Charnotskii, "Sparse spectrum model for a turbulent phase," *J. Opt. Soc. Am. A* **30**(3), 479 (2013).
33. D. A. Paulson, C. Wu, and C. C. Davis, "Randomized spectral sampling for efficient simulation of laser propagation through optical turbulence," *J. Opt. Soc. Am. B* **36**(11), 3249 (2019).
34. J. W. Strohbehn, *Modern Theories in the Propagation of Optical Waves in a Turbulent Medium, 45-106*, pp. 45–106, Springer Berlin Heidelberg (1978).
35. M. Faccioni, D. Kiehn, and P. Vrancken, "Quantifying the errors in modeling optical propagation in a turbulent atmosphere using different phase screen synthesization methods," *Proc. SPIE* **14150**, 141506Q (2026).
36. R. J. Noll, "Zernike polynomials and atmospheric turbulence," *J. Opt. Soc. Am.* **66**, 207 (1976).
37. N. Wiener, "Generalized harmonic analysis," *Acta Math.* **55**, 117–258 (1930).
38. A. D. Wheelon, *Electromagnetic Scintillation: Volume 1, Geometrical Optics*, Cambridge University Press (2010).
39. S. Gladysz et al., "Measuring non-Kolmogorov turbulence," *Proc. SPIE* **8890**, 889013 (2013).
40. H. A. Panofsky and J. A. Dutton, *Atmospheric Turbulence. Models and Methods for Engineering Applications*, John Wiley & Sons, Inc. (1984).
41. D. J. Thomson, "Spectrum estimation and harmonic analysis," *Proc. IEEE* **70**, 1055–1096 (1982).
42. J. W. Goodman, *Introduction to Fourier Optics*, McGraw-Hill (1996).

Matteo Faccioni is a PhD student at the German Aerospace Center (DLR). He received his BS and MS degrees in aerospace engineering, and MS degree in astrophysics from the University of Padua in 2018, 2020 and 2023, respectively. His current research interests include optical turbulence, atmospheric lidar, and interferometry.

Daniel Kiehn is a researcher at the DLR Institute of Flight Systems. He earned his BSc and an MSc degrees in mechanical engineering and aerospace engineering from RWTH Aachen University in 2014 and 2016, respectively. His current research focuses on lidar-based gust load alleviation and advanced flightcontrol concepts.

Biography of the other author is not available.